Biosensors and Bioelectronics 87 (2017) 970–975

Contents lists available at ScienceDirect

Biosensors and Bioelectronics

journal homepage: www.elsevier.com/locate/bios

Sensitive electrochemical assay of alkaline phosphatase activity based on TdT-mediated hemin/G-quadruplex DNAzyme nanowires for signal amplification

Yunqing Liu, Erhu Xiong, Xiaoyu Li, Junjing Li, Xiaohua Zhang*, Jinhua Chen*

State Key Laboratory of Chemo/Biosensing and Chemometrics, College of Chemistry and Chemical Engineering, Hunan University, Changsha 410082, PR China

ARTICLE INFO

Keywords:
Electrochemical biosensor
Hemin/G-quadruplex DNAzyme
Alkaline phosphatase
Terminal deoxynucletidyl transferase

ABSTRACT

Taking TdT-mediated hemin/G-quadruplex DNAzyme nanowires as NADH oxidase and HRP-mimicking DNAzyme, a novel DNA-based electrochemical method has been developed for sensitive and selective assay of alkaline phosphatase (AP) activity. The double-stranded DNA (dsDNA) probe consisted of thiol-functionalized DNA1 and 3′-phosphorylated DNA2, was immobilized on a gold nanoparticles (AuNPs) modified glassy carbon (GC) electrode. In the presence of AP, 3′-phosphoryl end of DNA2 was dephosphorylated. Terminal deoxynucletidyl transferase (TdT) catalyzed the sequential addition of deoxynucleotides (dTTPs) at 3′-OH end of DNA2 to extend DNA2 with a poly-T sequence. Then, G-rich DNA3 strand hybridized with the poly-T sequence of DNA2. Upon addition of hemin, the hemin/G-quadruplex DNAzyme was formed. In the presence of NADH, the hemin/G-quadruplex DNAzyme oxidased NADH to NAD^+, accompanied by the formation of H_2O_2 which was further catalyzed by hemin/G-quadruplex DNAzyme (served as a HRP-mimicking DNAzyme) with the thionine (Thi) as electron transfer mediator, leading to the amplified electrochemical signal. Under optimized conditions, the response peak current was linear with the concentration of AP in the range from 0.1 U L^{-1} to 5 U L^{-1} with the detection limit of 0.03 U L^{-1}. Also, the developed biosensor possessed good selectivity, reproducibility and stability, and simple sensing structure, showing promising practical applications in AP activity assay.

1. Introduction

Alkaline phosphatase (AP) is an enzyme that catalyzes the dephosphorylation process on a variety of substrates including nucleic acids, proteins, and small molecules (Coleman, 2003). As a common phosphatase in many organisms (Harris, 1990), AP is present in human tissues such as bone, liver, kidney, intestines, and placenta (Millán, 2006). The normal range of alkaline phosphatase is 20 to 140 U L^{-1} (Sharma et al., 2014). The abnormal level of AP has been proved to be associated with many diseases including breast and prostatic cancer, liver dysfunction, bone disease, and diabetes (Chen et al., 2014; Christenson, 1998; Ooi et al., 2007; Wolf, 1994). Thus, sensitive and selective assay of AP activity is highly desirable.

Till now, various methods have been developed to evaluate the activity of AP, such as colorimetry (Grates et al., 2003; Yang et al., 2016), chemiluminescence (Jiang and Wang, 2012), fluorescence (Chen et al., 2010; Freeman et al., 2010; Liu et al., 2009; Song et al., 2014; Zheng et al., 2014), surface Raman scattering (Ingram et al., 2009; Ruan et al., 2006) and electrochemical methods (Hassan et al., 2009; Ino et al., 2012; Zhang et al., 2015). However, some of the aforementioned methods required complicated and expensive instruments, which limits their applications in practical assay of AP activity. Among these methods, electrochemical assay has drawn considerable interest owing to its high sensitivity, good selectivity, low cost, and easy portability (Bhimji et al., 2013; Limoges et al., 2008;). Although some reported electrochemical methods have their own advantages in AP activity assay, there are still some defects such as relatively weak signals with low sensitivity, complex synthesis of AP substrates and sophisticated process with multiple tool enzymes (Miao et al., 2011; Zhang et al., 2015; Sean et al., 2015). Simple, sensitive and selective electrochemical method for AP activity assay is still desired.

To improve the sensitivity of the DNA-based electrochemical biosensors, many signal amplification strategies have been developed (Wu et al., 2014). Among them, a DNA polymerase called terminal deoxynucletidyl transferase (TdT) (Khan and Zharnikov, 2013) aroused our attention since it was template independent and could catalyze the

* Corresponding author.
E-mail addresses: mickyxie@hnu.edu.cn (X. Zhang), chenjinhua@hnu.edu.cn (J. Chen).

http://dx.doi.org/10.1016/j.bios.2016.09.069
Received 30 June 2016; Received in revised form 30 August 2016; Accepted 19 September 2016
Available online 20 September 2016

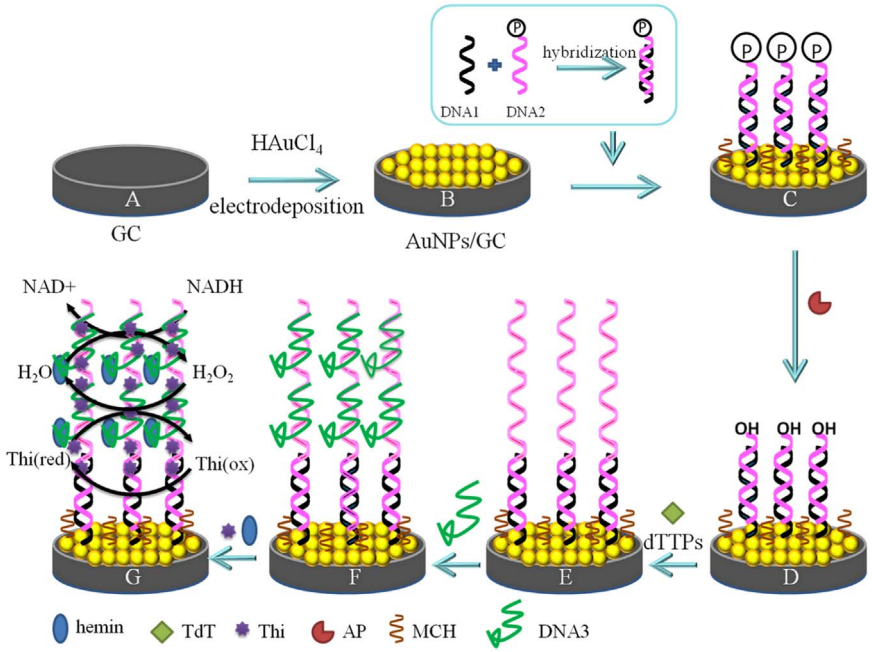

Scheme 1. Schematic illustration of DNA-based electrochemical biosensor for AP activity assay.

sequential addition of dNTPs at the 3′-OH group of an oligonucleotide primer to produce non-specific sequence. Hu et al. employed TdT to amplify the response signal in the target DNA detection (Hu et al., 2015). On the other hand, DNAzymes have been widely used to enhance the assay sensitivity of electrochemical biosensors (Liu et al., 2013; Wu et al., 2015; Yuan et al., 2014a). One of the interesting DNAzymes, hemin/G-quadruplex DNAzyme, has been reported to be simultaneously served as an NADH oxidase and HRP-mimicking DNAzyme (Golub et al., 2011). Yuan et al. reported sensitive detection of mercury (II) based on the excellent catalytic activity of an autonomously assembled hemin/G-quadruplex DNAzyme nanowires (Yuan et al., 2014b).

Here in, taking TdT to introduce lots of hemin/G-quadruplex DNAzymes, we developed a sensitive and selective DNA-based electrochemical biosensor for AP activity assay. As illustrated in Scheme 1, a double-stranded DNA (dsDNA) probe was prepared by hybridizing the thiol-functionalized DNA1 with the 3′-phosphorylated DNA2. Then, the obtained dsDNA was immobilized on gold nanoparticles (AuNPs)-modified glassy carbon (GC) electrode through a strong thiol-gold (Au-S) bond between AuNPs and the thiol group of DNA1. In the presence of AP, 3′-phosphoryl end of DNA2 was dephosphorylated. TdT catalyzed the sequential addition of deoxynucleotides (dTTPs) at 3′-OH end of DNA2 to extend DNA2 with a poly-T sequence. Then, G-rich DNA3 strand hybridized with the poly-T sequence. Upon addition of hemin, hemin/G-quadruplex DNAzyme was formed. The hemin/G-quadruplex DNAzyme oxidased NADH to NAD^+ with the concomitant formation of H_2O_2 which was further catalytically reduced by hemin/G-quadruplex DNAzyme nanowires (served as a HRP-mimicking DNAzyme) with thionine (Thi) as electron mediator, leading to the enhanced electrochemical signal. The related mechanism is as follows (Yuan et al., 2012):

$$Fe(III)+NADH \rightarrow Fe(II)+NAD\cdot+H^+$$

$$Fe(II)+NAD\cdot+H^+ +O_2 \rightarrow NAD^+ +Fe(III)\text{-}OOH$$

$$Fe(III)\text{-}OOH+H^+ \rightarrow H_2O_2+Fe(III)$$

$$H_2O_2+Fe(III) \rightarrow Fe(II)+H_2O+O_2$$

$$Fe(II)+ThiH \rightarrow Fe(III)+ThiH^+ +2e$$

$$ThiH^+ +H^+ +2e \rightarrow ThiH_2$$

Thus, AP activity was sensitively and selectively evaluated. Also, the proposed electrochemical biosensor showed low detection limit and good reproducibility.

2. Experimental section

2.1. Materials and instruments

Shrimp alkaline phosphatase and Terminal transferase (TdT) were obtained from New England Biolabs, Ltd (Beijing, China). Deoxythymine triphosphate (dTTP) was purchased from Thermo scientific (Shanghai, China). The sterile-filtered and heat-inactivated normal human serum was purchased from Anyan Inc. (Shanghai, China).

The oligonucleotides used in this work were HPLC-purified and synthesized by Sangon Biotechnology Co. Ltd. (Shanghai, China). The sequences of the oligonucleotides were listed as follows:

DNA1, 5′-GTT CAT GCC GCC CAT GCT-SH-3′
DNA2, 5′-ATG GGC GGC ATG AAC-P-3′
DNA3, 5′-GGG TAG GGC GGG TTG GGC TTT AAA AAA AAA AAA AAA-3′

6-Mercaptohexanol (MCH) and tris (2-carboxyethyl) phosphine hydrochloride (TCEP) were purchased from Sigma-Aldrich. Tris-(hydroxymethyl)aminomethane (Tris) was purchased from Solarbio Science & technology Co., Ltd. (Beijing, China). NaCl, KCl, KH_2PO_4, $Na_2HPO_4{\cdot}12H_2O$, $HAuCl_4{\cdot}4H_2O$, H_2SO_4 and EDTA were purchased from Sinopharm Chemical Reagent Co., Ltd (China). Thi was purchased from J & K Scientific Ltd. (Beijing, China). Nicotinamide adenine dinucleotide (NADH) was purchased from Genview (Genview, scientific Inc., USA). Hemin was purchased from Shanghai Ryon Biological Technology Co., ltd. (Shanghai, China). All chemicals were of analytical grade. Aqueous solutions were prepared by ultrapure water obtained from a Milli-Q water purification system (Millipore Corp., Bedford, MA).

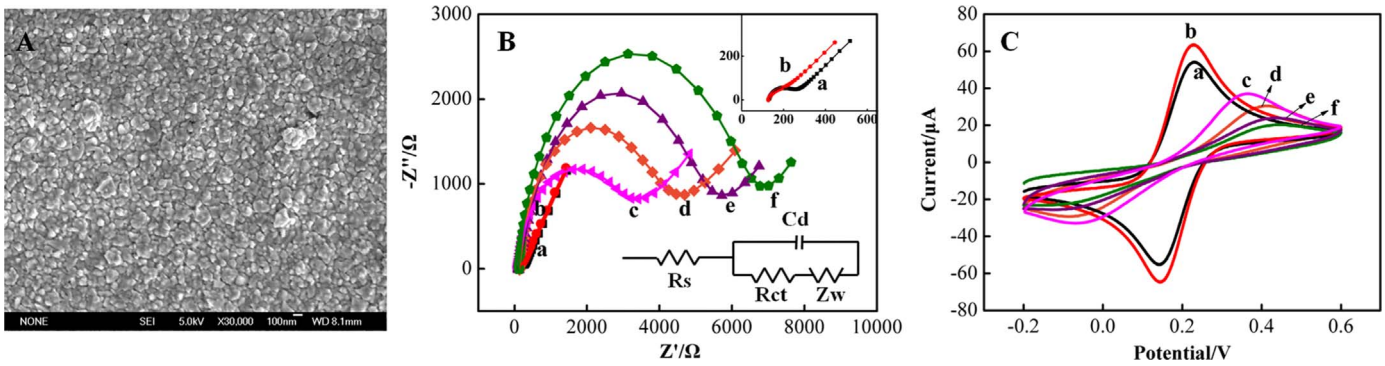

Fig. 1. (A) SEM image of AuNPs-modified GC electrode. (B) Electrochemical impedance spectra (Nyquist plots) (the solid line implies the fitting results) and (C) cyclic voltammograms of the different electrodes in $[Fe(CN)_6]^{3-/4-}$ (5 mM)+ KCl (0.1 M) aqueous solution. The impedance spectra were recorded in the range of 0.1 Hz–100 kHz with AC amplitude of 5 mV and cyclic voltammetry experiments were performed at a scan rate of 100 mV s^{-1}. (a) bare GC, (b) AuNPs/GC, (c) dsDNA/AuNPs/GC, (d) MCH/dsDNA/AuNPs/GC, (e) MCH/dsDNA/AuNPs/GC incubated with AP and TdT+dTTPs, (f) (e) incubated with DNA3. Inset plots of figure B, equivalent circuit model for electrochemical impedance measurement system (the lower right corner) and the Nyquist plots of the bare GC (a) and AuNPs/GC (b) electrodes (the upper right corner).

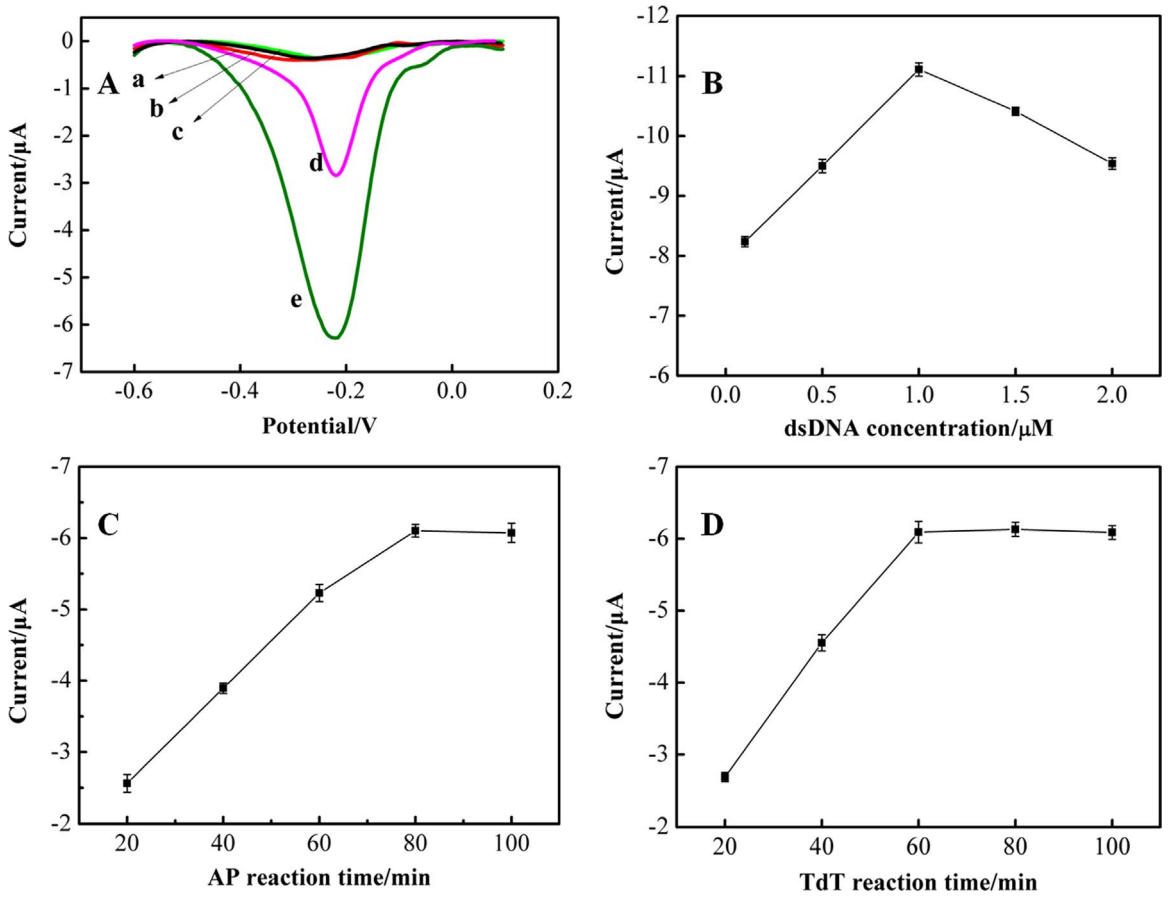

Fig. 2. (A) DPV responses in the absence of AP (a), TdT+dTTPs (b), AP and TdT+dTTPs (c), in the presence of both 3 U L^{-1}AP and 0.5 U μL^{-1} TdT+10 mM dTTPs without hemin (d) and with 0.15 mM hemin (e) in 0.1 M PBS (pH 7.0) containing 3 mM NADH. DPV response peak currents depend on the concentration of dsDNA probes (both of the reaction times of AP and TdT, 60 min) (B), reaction times of AP (AP concentration, 3 U L^{-1}; dsDNA concentration, 1.0 μM; reaction time of TdT, 60 min) (C) and TdT (TdT concentration, 0.5 U μL^{-1}; dsDNA concentration, 1.0 μM; reaction time of AP, 80 min) (D) in 0.1 M PBS (pH 7.0) containing 3 mM NADH.

The morphology of the electrode was characterized by scanning electron microscopy (SEM, JSM-6700, JEOL Ltd. Japan). All electrochemical measurements, including cyclic voltammetry (CV) and differential pulse voltammetry (DPV), were carried out on a CHI 660A Electrochemical Workstation (Chenhua Instrument Company of Shanghai, China). Electrochemical impedance spectroscopy (EIS) results were obtained on Zahner Electrochemical Workstation (Im6ex, Zahner-Elektrik Gmbh & Co. KG, Germany). A conventional three–electrode system was used with a glassy carbon (GC) electrode (3 mm) as the working electrode, a platinum wire as the counter electrode and a saturated calomel electrode (SCE) as the reference electrode. All potentials in this paper were referred to SCE.

2.2. Preparation of the electrochemical biosensor

Before use, the GC electrode was polished carefully to a mirror-like surface with 0.5 and 0.05 μm alumina slurries, followed by ultrasonication in ultra pure water and ethanol. The electrode was further treated by electrochemical oxidation and reduction in 0.5 M H_2SO_4 aqueous solution by potential cycling in the potential range from −0.2

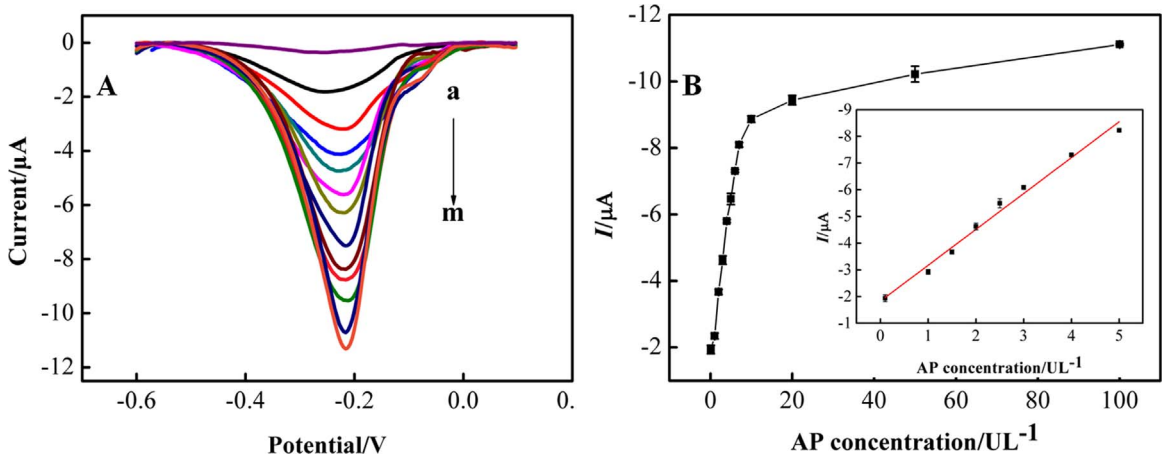

Fig. 3. (A) DPV responses of the developed method to different concentration of AP (from a to m): 0, 0.1, 1, 1.5, 2, 2.5, 3, 4, 5, 10, 50, 100 and 500 U L^{-1} in 0.1 M PBS (pH 7.0) containing 3 mM NADH. (B) Dependence of *I* on AP concentration.

Table 1
Comparison of the different methods for AP detection.

Methods	Detection limit (U L^{-1})	References
Colorimetry	0.83	Yang et al. (2016)
Chemiluminescence	2	Jiang and Wang (2012)
Fluorescence	40	Song et al. (2016)
	0.15	Song et al. (2014)
	100	Zheng et al. (2014)
Surface Raman scattering	30	Ruan et al. (2006)
Electrochemistry	100	Miao et al., (2011)
	0.1	Zhang et al. (2015)
	0.4	Sean et al. (2015)
	0.03	This work

to 1.2 V with a scan rate of 100 mV s^{-1}. The purpose of this kind of treatment for GC electrode surface is to improve the hydrophilicity of the electrode surface, which is beneficial to the deposition of AuNPs on the GC electrode surface. Then, the GC electrode was washed with copious amounts of ultra pure water and dried under nitrogen gas. After that, the pretreated electrode was immersed in a 24.3 mM chloroauric acid solution and kept at the potential of −0.2 V for 1 min to electrodeposit AuNPs (Hou et al., 2016; Liu et al., 2016; Xu et al., 2015;) The obtained electrode was rinsed with ultrapure water, allowed to dry with nitrogen gas, and denoted as AuNPs/GC.

Before the hybridization with DNA2, the DNA1 was firstly dissolved in 10 mM Tris-HCl buffer solution (containing 1 M NaCl, 1 mM EDTA, 1 mM TCEP, pH 7.0) and incubated in the dark for 1 h to reduce disulfide bunds. After that, DNA1 (50 μL, 2 μM) and DNA2 (50 μL, 2 μM) were mixed, incubated at 95 °C for 5 min and cooled down to room temperature to obtain the dsDNA probe. The dsDNA/AuNPs/GC electrode was prepared by dropping 10 μL dsDNA solution onto the AuNPs/GC electrode surface for 16 h. The above electrode was further immersed into 10 mM Tris-HCl buffer with 1 mM MCH for 1 h to block the uncovered AuNPs/GC electrode surface and labeled as MCH/dsDNA/AuNPs/GC electrode. Each immobilization step was monitored by the electrochemical impedance measurements which were performed in 0.1 M KCl aqueous solution with 5 mM $[Fe(CN)_6]^{3-/4-}$ as the probe in the frequency range from 0.1 to 100 kHz with 5 mV as the amplitude at a potential of 0.22 V (vs. SCE).

2.3. Electrochemical measurements

The MCH/dsDNA/AuNPs/GC electrode was incubated in 1×CutSmart buffer containing varies concentrations of AP at 37 °C for 80 min. After rinsed with Tris-HCl buffer, the electrode was incubated with 1×TdT reaction buffer containing 0.5U μL^{-1} TdT and 10 mM dTTP at 37 °C for 60 min to get the DNA2 extended. Then, the DNA3 was placed on the above electrode for 60 min to achieve the hybridization between DNA3 and poly-T sequence of DNA2, yielding DNA3/MCH/dsDNA/AuNPs/GC electrode. Subsequently, the electrode was immersed in 0.15 mM hemin for 60 min to form the hemin/G-quadruplex complex and then incubated with 0.25 mM Thi for 60 min. Finally, the electrochemical performance of the above electrode was investigated by DPV in 0.1 M PBS (pH 7.0) containing

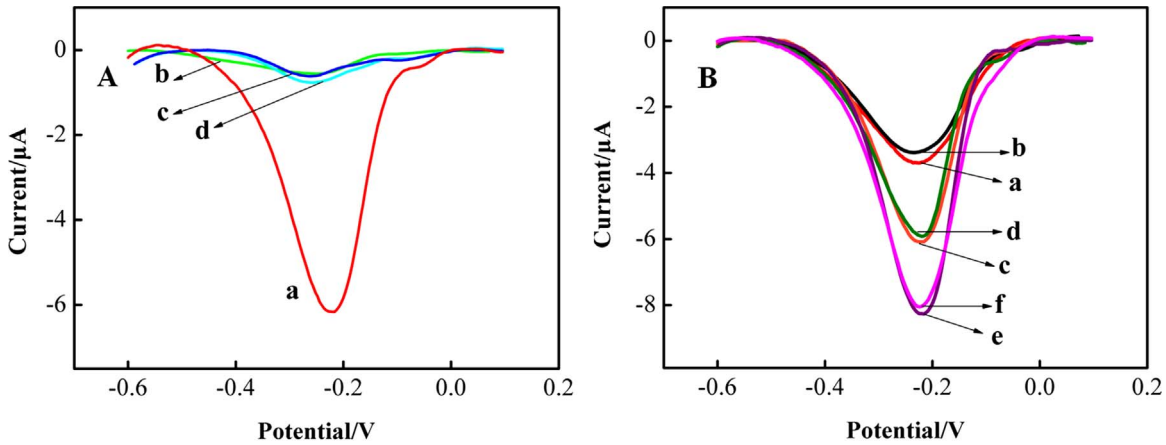

Fig. 4. (A) Selectivity of the developed biosensor for AP (a), BSA (b), Lysozyme (c), and Pepsin (d). (B) Comparison of the AP concentration assay in 1×CutSmart buffer (a, c, e) and normal human serum samples (b, d, f). The concentration of AP, 1.5 U L^{-1} (a, b); 3.0 U L^{-1} (c, d); 5.0 U L^{-1} (e, f).

3 mM NADH in the potential range from −0.6 to 0.1 V with amplitude 0.05 V, pulse width 0.05 s, and sample width 0.0167 s.

3. Results and discussion

3.1. Characterization of the developed biosensor

Fig. 1A shows the SEM image of the AuNPs/GC electrode. It is noted that there are lots of AuNPs on the GC electrode, which is beneficial to the immobilization of DNA probes.

On the other hand, it is well-known that electrochemical impedance spectroscopy (EIS) is widely used to study the interface properties of the modified electrodes (Bardea et al., 1999). The preparation of the biosensor was characterized by EIS and the corresponding results are shown in Fig. 1B. The impedance spectra were modeled with the Randles's equivalent circuit approach (as shown in the inset of Fig. 1B) (Radi et al., 2005), and the fitting values of all parameters are shown in Fig. S1 and Table S1 (see Supplementary material section). Among all parameters, the interfacial charge-transfer resistance (R_{ct}) is the most directive and sensitive parameter that responds to the changes of the electrode interface (Cao et al., 2012; Li et al., 2005; Xu et al., 2005). As shown in Fig. 1B, the bare GC electrode shows a small semicircle domain (R_{ct}=125 Ω, curve a, Fig. 1B). After the electrodeposition of AuNPs on the GC electrode, a smaller R_{ct} (79 Ω, curve b, Fig. 1B) is observed, indicating that AuNPs accelerate the interfacial electron transfer between the $[Fe(CN)_6]^{3-/4-}$ redox probe and the GC electrode surface. Subsequent self-assembly of dsDNA on the AuNPs/GC electrode leads to the increase of R_{ct} value obviously (3172 Ω, curve c, Fig. 1B). The main reasons should be the effective repulsion between the negatively charged dsDNA and $[Fe(CN)_6]^{3-/4-}$ and steric hinerance effect. From curve d in Fig. 1A, it is noted that the surface blocking with MCH induces a further increase of R_{ct} value (4084 Ω). After incubation with AP and TdT + dTTPs, the R_{ct} value increases to 5815 Ω (curve e, Fig. 1B) due to the addition of poly-T sequence to 3′-OH termini of DNA2. When the electrode is further incubated with DNA3, the R_{ct} value increases to 6836 Ω (curve f, Fig. 1B), implying the successful hybridization between DNA3 and the poly-T sequence of DNA2, and the formation of the DNA3/MCH/dsDNA/AuNPs/GC electrode.

In order to further verify the stepwise modification process, the electrodes were also characterized by CV and the corresponding results are shown in Fig. 1C. The values of peak currents and peak potentials of different CV curves are shown in Table S2 (see Supplementary material section). As shown in Fig. 1C and Table S2, compared with the bare GC electrode (curve a, Fig. 1C), the peak currents of the AuNPs/GC electrode (curve b, Fig. 1C) increase and the corresponding potential difference decreases. This implies that AuNPs can enhance the electron-transfer properties of the electrode and the reversibility of the redox process of $[Fe(CN)_6]^{3-/4-}$ probe increases. After the self-assembly of dsDNA, the peak currents decrease correspondingly (curve c, Fig. 1C). When the surface of the dsDNA/AuNPs/GC electrode is blocked by MCH, further decreased redox peak currents (curve d, Fig. 1C) are obtained. After the incubation of MCH/dsDNA/AuNPs/GC electrode with AP and TdT + dTTPs, the peak currents of the electrode decrease again, due to the addition of poly-T sequence to the 3′-OH termini of DNA2 (curve e, Fig. 1C). When DNA3 hybridizes with the poly-T sequence of DNA2, the peak currents of the electrode further decrease (curve f, Fig. 1C). Also, the potential difference increases from curve b to curve f, implying that the reversibility of the redox process of $[Fe(CN)_6]^{3-/4-}$ probe decreases. These results are in accordance with that observed in EIS investigation (Fig. 1B) and demonstrate that the electrochemical biosensor has been fabricated successfully according to Scheme 1.

3.2. Feasibility of the developed biosensor

To investigate the feasibility of the proposed biosensor for AP activity assay, DPV experiments were carried out and the corresponding results are shown in Fig. 2A. In the absence of AP (curve a, Fig. 2A) or TdT+dTTPs (curve b, Fig. 2A) only and AP and TdT+dTTPs both (curve c, Fig. 2A), no obvious DPV peak currents are obtained due to the lack of dephosphorylation reaction or the sequence extension. With the addition of both AP and TdT+dTTPs (curves d and e, Fig. 2A), significant DPV peak currents are observed. As is shown, the peak current of curve e (with hemin) is much larger than that of curve d (without hemin). It suggests the excellent catalytic effects of the hemin/G-quadruplex DNAzyme nanowires. The above results clearly indicate that the developed biosensor could be adopted for AP activity assay.

3.3. Optimization of experimental conditions

The surface concentration of the immobilized dsDNA probes, the reaction time of AP and the reaction time of TdT-mediated extension were optimized. Fig. 2B indicates the highest response peak current is reached when the concentration of dsDNA probes is 1 μM. With the further increase of the dsDNA concentration, the DPV response peak current decreases. The possible reason may be that the higher dsDNA probe density on the electrode surface will negatively influence the catalytic efficiency of AP and TdT because of the steric hinerance effect of dsDNA. Therefore, the optimal concentration of dsDNA is chosen as 1 μM. On the other hand, as shown in Fig. 2C, the DPV response peak current increases with the increase of the AP reaction time. After the AP reaction time is more than 80 min, the DPV response peak current does not change obviously. Similarly, for TdT-mediated extension reaction, DPV response peak current reaches a maximum value at about 60 min and then no obvious change is observed (Fig. 2D). Thus, in the subsequent experiments, 80 and 60 min are selected as the optimal reaction time for AP and TdT, respectively.

3.4. Assay performance

The performance of proposed biosensor was investigated by DPV with various concentration of AP under the optimal experimental conditions. It is noted that DPV peak current increases with the increase of AP concentration (Fig. 3A). The dependence of the peak current (I) on the AP concentration is shown in Fig. 3B. It is noted that the value of I is linear with the concentration of AP in the range from 0.1 U L^{-1} to 5 U L^{-1} with the detection limit of 0.03 U L^{-1} (3σ), and the linear regression equation is I=−1.35295 C−1.79771 (R^2=0.98795). To our best knowledge, the obtained detection limit (0.03 U L^{-1}) is much lower than those obtained by some reported methods (Table 1). The low detection limit may bring benefit to a low sampling quantity, which has great advantages in clinical assay.

3.5. Selectivity, reproducibility and stability of the biosensor

It is well-known that all phosphatases from different families, such as AP, PTEN (phosphatase and tensin homolog deleted on chromosome ten), PTP1B (proteintyrosine phosphatase-1B) and PP2A (protein phosphatase 2A), are able to dephosphorylate the phosphoryl into hydroxyl. Therefore, control experiments were performed for some non-phosphatase interfering proteins, such as BSA, Lysozyme and pepsin, to evaluate the selectivity of the proposed biosensor in a complex system. The concentrations of the interfering proteins are much higher than that of AP. As shown in Fig. 4A and Fig. S2A (see Supplementary material section), the response signals caused by BSA, Lysozyme and pepsin are very small, while the AP gives obvious change of the electrochemical signal. Therefore, the developed biosensor exhibits good performance for discriminating AP against other interfering proteins.

The reproducibility and stability of the proposed biosensor were also investigated. Five different electrodes were used to detect AP (2.5 U L^{-1}) and the relative standard deviation is 4.9%. Furthermore,

the response peak current of the developed biosensor has no significant change after 15-d storage at 4 °C. These results demonstrate that the proposed biosensor exhibits satisfactory reproducibility and stability.

3.6. AP assay in biological fluids

The developed biosensor was utilized to detect AP in the sterile-filtered and heat-inactivated normal human serum samples without active AP to further evaluate its practical application in complex system. AP solutions with different concentrations (1.5 U L^{-1}, 3 U L^{-1}, 5 U L^{-1}) were added in 10-fold diluted human serum sample solutions diluted with 20 mM PBS. Figs. 4B and S2B (see Supplementary material section) reveal that the DPV response peak currents to AP spiked in normal human serum samples are almost same with that to AP spiked in 1×CutSmart buffer, implying that the proposed method may become a promising approach for AP activity assay in real biological fluids.

4. Conclusion

Based on the excellent electrocatalytic recycling signal amplification properties of TdT-mediated hemin/G-quadruplex DNAzyme nanowires, a novel DNA-based electrochemical biosensor has been developed for sensitive and selective assay of AP activity. The dsDNA probe consisted of thiol-functionalized DNA1 and 3′-phosphorylated DNA2, is immobilized on the AuNPs-modified GC electrode. In the presence of AP, 3′-phosphoryl end of DNA2 is dephosphorylated. Then, TdT catalyzes the sequential addition of deoxynucleotides (dTTPs) at 3′-OH end of DNA2 to extend DNA2 with a poly-T sequence. After the hybridization between G-rich DNA3 strand and the poly-T sequence of DNA2, and the addition of hemin, the hemin/G-quadruplex DNAzyme nanowires form and serve as a catalyst to oxidize NADH to NAD^+ with the concomitant formation of H_2O_2. With the Thi as electron mediator, the hemin/G-quadruplex DNAzyme nanowires act as HRP-mimicking DNAzyme to further catalytically reduce H_2O_2, leading to the enhanced electrochemical response signal. Based on the developed biosensor, AP can be detected sensitively and selectively with a linear range from 0.1 U L^{-1} to 5 U L^{-1} and a detection limit of 0.03 U L^{-1}. The detection limit is much lower than that obtained by most of the reported methods. The developed method also shows good applicability in AP activity assay in human serum samples, and excellent reproducibility and stability. Other biosensors could also be designed using the similar principles to detect a wide spectrum of analytes (such as protein, DNA and RNA). The strategy developed in this paper has great potential for the development of ultrasensitive biosensing platform for early diagnosis.

Acknowledgements

This work was financially supported by NSFC (21475035, 21235002, 21275041), the Foundation for Innovative Research Groups of NSFC (21521063), and PCSIRT (IRT1238).

Appendix A. Supporting information

Supplementary data associated with this article can be found in the online version at doi:10.1016/j.bios.2016.09.069.

References

Bardea, A., Patolsky, F., Dagan, A., Willner, I., 1999. Chem. Commun. 1, 21–22.
Bhimji, A., Zaragoza, A.A., Live, L.S., Kelley, S.O., 2013. Anal. Chem. 85 (14), 6813–6819.
Cao, Y., Zhu, S., Yu, J., Zhu, X., Yin, Y., Li, G., 2012. Anal. Chem. 84 (10), 4314–4320.
Chen, Q., Bian, N., Cao, C., Qiu, X.L., Qi, A.D., Han, B.H., 2010. Chem. Commun. 46 (23), 4067–4069.
Chen, L., Li, X., Zheng, Z., Lu, X., Lin, M., Pan, C., Liu, J., 2014. Gene 538 (1), 204–206.
Christenson, R.H., 1998. Clin. Biochem 30 (8), 573–593.
Coleman, J.E., 2003. Annu. Rev. Biophys. Biomol. Struct. 21 (1), 441–483.
Freeman, R., Finder, T., Gill, R., Willner, I., 2010. Nano Lett. 10 (6), 2192–2196.
Grates, H.E., Mcgowen, R.M., Gupta, S.V., Falck, J.R., Brown, T.R., 2003. J. Biosci. 28 (1), 109–113.
Golub, E., Freeman, R., Willner, I., 2011. Angew. Chem. Int. Ed. 50 (49), 11710–11714.
Harris, H., 1990. Clin. Chim. Acta 186 (2), 133–150.
Hassan, S.S.M., Sayour, H.E.M., Kamel, A.H., 2009. Anal. Chim. Acta 640 (1–2), 75–81.
Hou, L., Ding, Y., Guo, Y., Li, M., Chen, Z., Wu, X., 2016. Sens. Actuators B-Chem. 233, 63–67.
Hu, Y., Shen, Q., Li, W., Liu, Z., Nie, Z., Yao, S., 2015. Biosens. Bioelectron. 63, 331–338.
Ingram, A., Moore, B.D., Graham, D., 2009. Bioorg. Med. Chem. Lett. 19 (6), 1569–1571.
Ino, K., Kanno, Y., Arai, T., Inoue, K.Y., Takahashi, Y., Shiku, H., Matsue, T., 2012. Anal. Chem. 84 (18), 7593–7598.
Jiang, H., Wang, X., 2012. Anal. Chem. 84 (16), 6986–6993.
Khan, M.N., Zharnikov, M., 2013. J. Phys. Chem. C 117 (47), 24883–24893.
Li, C.Z., Liu, Y., Luong, J.H., 2005. Anal. Chem. 77 (2), 478–485.
Limoges, B., Marchal, D., Mavré, F., Savéant, J.M., Schöllhorn, B., 2008. J. Am. Chem. Soc. 130 (23), 7259–7275.
Liu, J.M., Huang, X.M., Liu, Z.B., Lin, S.Q., Li, F.M., Gao, F., Li, Z.M., Zeng, L.Q., Li, L.Y., Ouyang, Y., 2009. Anal. Chim. Acta 648 (2), 226–234.
Liu, S., Wang, C., Zhang, C., Wang, Y., Tang, B., 2013. Anal. Chem. 85 (4), 2282–2288.
Liu, Y., Zhang, X., Yang, J., Xiong, E., Zhang, X., Chen, J., 2016. Can. J. Chem. 94 (5), 509–514.
Miao, P., Ning, L., Li, X., Shu, Y., Li, G., 2011. Biosens. Bioelectron. 27 (1), 178–182.
Millán, J.L., 2006. Purinergic Signal. 2 (2), 335–341.
Ooi, K., Shiraki, K., Morishita, Y., Nobori, T., 2007. J. Clin. Lab Anal. 21 (3), 133–139.
Radi, A., Acero Sanchez, J., Baldrich, E., O'Sullivan, C., 2005. Anal. Chem. 77, 6320–6323.
Ruan, C., Wang, W., Gu, B., 2006. Anal. Chem. 78 (10), 3379–3384.
Sean, G., Christophe, N., Barrie, J., Marsh, Christopher, G., 2015. Chem. Commun. 51, 561–564.
Sharma, U., Pal, D., Prasad, R., 2014. Indian J. Clin. Biochem. 29 (3), 269–278.
Song, Z., Kwok, R.T., Zhao, E., He, Z., Hong, Y., Lam, J.W., Liu, B., Tang, B.Z., 2014. ACS Appl. Mater. Interfaces 6 (19), 17245–17254.
Song, C., Yang, X., Wang, K., Wang, Q., Liu, J., Huang, J., Zhou, M., Guo, X., 2016. Spectrochim. Acta A 156, 131–137.
Wolf, D.P.L., 1994. J. Clin. Lab Anal. 8 (3), 172–176.
Wu, L., Xiong, E., Zhang, X., Zhang, X., Chen, J., 2014. Nano Today 9 (2), 197–211.
Wu, S.H., Tang, Y., Chen, L., Ma, X.G., Tian, S.-M., Sun, J.J., 2015. Biosens. Bioelectron. 73, 41–46.
Xu, D., Xu, D., Yu, X., Liu, Z., He, W., Ma, Z., 2005. Anal. Chem. 77 (16), 5107–5113.
Xu, W., Yi, H., Yuan, Y., Jing, P., Chai, Y., Yuan, R., 2015. Biosens. Bioelectron. 64, 423–428.
Yang, J., Zheng, L., Wang, Y., Li, W., Zhang, J., Gu, J., Fu, Y., 2016. Biosens. Bioelectron. 77, 549–556.
Yuan, L., Tu, W., Bao, J., Dai, Z., 2014a. Anal. Chem. 87 (1), 686–692.
Yuan, Y., Gao, M., Liu, G., Chai, Y., Wei, S., Yuan, R., 2014b. Anal. Chim. Acta 811, 23–28.
Yuan, Y., Yuan, R., Chai, Y., Zhuo, Y., Ye, X., Gan, X., Bai, L., 2012. Chem. Commun. 48, 4621–4623.
Zhang, L., Hou, T., Li, H., Li, F., 2015. Analyst 140 (12), 4030–4036.
Zheng, F., Guo, S., Zeng, F., Li, J., Wu, S., 2014. Anal. Chem. 86 (19), 9873–9879.